



SOA from aqueous reactions of phenols with two oxidants

L. Yu et al.

This discussion paper is/has been under review for the journal Atmospheric Chemistry and Physics (ACP). Please refer to the corresponding final paper in ACP if available.

# Chemical characterization of SOA formed from aqueous-phase reactions of phenols with the triplet excited state of carbonyl and hydroxyl radical

L. Yu<sup>1</sup>, J. Smith<sup>2</sup>, A. Laskin<sup>3</sup>, C. Anastasio<sup>2</sup>, J. Laskin<sup>4</sup>, and Q. Zhang<sup>1</sup>

<sup>1</sup>Department of Environmental Toxicology, University of California, 1 Shields Ave., Davis, CA 95616, USA

<sup>2</sup>Department of Land, Air and Water Resources, University of California, 1 Shields Ave., Davis, CA 95616, USA

<sup>3</sup>Environmental Molecular Sciences Laboratory, Pacific Northwest National Laboratory, Richland, WA 99352, USA

<sup>4</sup>Physical Sciences Division, Pacific Northwest National Laboratory, Richland, WA 99352, USA

Received: 3 August 2014 – Accepted: 4 August 2014 – Published: 19 August 2014

Correspondence to: Q. Zhang (dkwzhang@ucdavis.edu)

Published by Copernicus Publications on behalf of the European Geosciences Union.

Title Page

Abstract

Introduction

Conclusions

References

Tables

Figures



Back

Close

Full Screen / Esc

Printer-friendly Version

Interactive Discussion



## Abstract

Phenolic compounds, which are emitted in significant amounts from biomass burning, can undergo fast reactions in atmospheric aqueous phases to form secondary organic aerosol (aqSOA). In this study, we investigate the reactions of phenol and two methoxyphenols (syringol and guaiacol) with two major aqueous phase oxidants – the triplet excited states of an aromatic carbonyl ( $^3C^*$ ) and hydroxyl radical ( $\cdot OH$ ). We thoroughly characterize the low-volatility species produced from these reactions and interpret their formation mechanisms using aerosol mass spectrometry (AMS), nanospray desorption electrospray ionization mass spectrometry (nano-DESI MS), and ion chromatography (IC). A large number of oxygenated molecules are identified, including oligomers containing up to six monomer units, functionalized monomer and oligomers with carbonyl, carboxyl, and hydroxyl groups, and small organic acid anions (e.g., formate, acetate, oxalate, and malate). The average atomic oxygen-to-carbon (O/C) ratios of phenolic aqSOA are in the range of 0.85–1.23, similar to those of low-volatility oxygenated organic aerosol (LV-OOA) observed in ambient air. The aqSOA compositions are overall similar for the same precursor, but the reactions mediated by  $^3C^*$  are faster than  $\cdot OH$ -mediated reactions and produce more oligomers and hydroxylated species at the point when 50% of the phenol had reacted. Profiles determined using a thermodenuder indicate that the volatility of phenolic aqSOA is influenced by both oligomer content and O/C ratio. In addition, the aqSOA shows enhanced light absorption in the UV-vis region, suggesting that aqueous-phase reactions of phenols are likely an important source of brown carbon in the atmosphere, especially in regions influenced by biomass burning.

## 1 Introduction

Secondary organic aerosol (SOA) is ubiquitous in the atmosphere (Murphy et al., 2006; Zhang et al., 2007; Jimenez et al., 2009) and plays an important role in climate, human

ACPD

14, 21149–21187, 2014

## SOA from aqueous reactions of phenols with two oxidants

L. Yu et al.

Title Page

Abstract

Introduction

Conclusions

References

Tables

Figures



Back

Close

Full Screen / Esc

Printer-friendly Version

Interactive Discussion



**SOA from aqueous reactions of phenols with two oxidants**

L. Yu et al.

[Title Page](#)[Abstract](#)[Introduction](#)[Conclusions](#)[References](#)[Tables](#)[Figures](#)[Back](#)[Close](#)[Full Screen / Esc](#)[Printer-friendly Version](#)[Interactive Discussion](#)

health, and air quality. Thus understanding the impacts of SOA requires a thorough knowledge of the formation, evolution, and composition of SOA. This knowledge, however, is still limited because atmospheric organic chemistry is extremely complex. Numerous sources emit organic compounds and organic aerosol is formed and transformed via complicated chemical and physical processes in the atmosphere (Kanakidou et al., 2005).

SOA formation can take place in both gas and condensed phases. Much of the previous research on SOA has mainly focused on gas-phase reactions of volatile organic compounds (Hallquist et al., 2009). Recent work, however, has shown that SOA can also be produced efficiently in cloud and fog drops and water-containing aerosol (Blando and Turpin, 2000; Lim et al., 2005; Altieri et al., 2006; Ervens et al., 2011). Understanding the characteristics of SOA formed from aqueous-phase reactions (aq-SOA) is important for properly representing its formation pathways in models and for elucidating its climatic and health effects.

Phenols are important precursors of aqSOA because (1) they are emitted in large quantities from biomass burning (Hawthorne et al., 1989; Schauer et al., 2001); (2) they have high Henry's Law constants and can partition significantly into atmospheric aqueous phases (Sagebiel and Seiber, 1993; Sander, 1999); and (3) they can undergo fast reactions with hydroxyl radical ( $\cdot\text{OH}$ ) and triplet excited states of organic compounds ( $^3\text{C}^*$ ) formed via light absorption by dissolved chromophores (Anastasio et al., 1997; Canonica et al., 2000; Smith et al., 2014). In the aqueous phase,  $\cdot\text{OH}$  is typically considered a dominant oxidant for organics. However, a recent study by Smith et al. (2014) showed that the destruction rates of phenols by  $^3\text{C}^*$  are comparable to or faster than those by  $\cdot\text{OH}$  under typical ambient conditions in areas influenced by biomass burning. An important source of  $^3\text{C}^*$  in the atmosphere is non-phenolic aromatic carbonyls – a group of compounds that are emitted from wood combustion in significant amounts (Hawthorne et al., 1992; Simoneit et al., 1999) and have been detected in fog and cloud droplets (Leuenberger et al., 1985; Sagebiel and Seiber, 1993). These compounds, once dissolved in water, can catalyze the photooxidation of

phenols and generate aqSOA with little or no loss of the aromatic carbonyl (Anastasio et al., 1997; Smith et al., 2014).

Recent studies have shown that phenols react with  $\cdot\text{OH}$  and  $^3\text{C}^*$  to form aqSOA with mass yields close to 100% (Smith et al., 2014) and that the reaction products include small organic acids, hydroxylated phenols, and oligomers (Sun et al., 2010). However, since Sun et al. (2010) mainly used an Aerodyne high-resolution time-of-flight aerosol mass spectrometer with an electron impact (EI) ionization source, in which analyte molecules are generally extensively fragmented (Canagaratna et al., 2007), the molecular composition of the phenolic aqSOA was not sufficiently characterized. In addition, almost nothing is known about the chemistry of aqSOA formed from  $^3\text{C}^*$  reactions.

In this study, we thoroughly characterize the aqueous reaction products of phenols with  $^3\text{C}^*$  produced from a non-phenolic aromatic carbonyl and  $\cdot\text{OH}$  from hydrogen peroxide (HOOH) under simulated sunlight illumination. We studied three basic structures of biomass-burning phenols – phenol ( $\text{C}_6\text{H}_6\text{O}$ ), guaiacol ( $\text{C}_7\text{H}_8\text{O}_2$ ; 2-methoxyphenol), and syringol ( $\text{C}_8\text{H}_{10}\text{O}_3$ ; 2,6-dimethoxyphenol). We examine the molecular and bulk compositions of low-volatility species produced from these reactions and use this information to interpret the formation pathways of phenolic aqSOA.

## 2 Experimental Methods

### 2.1 Phenolic aqSOA samples

The aqSOA samples of phenol, guaiacol, and syringol were prepared during simulated sunlight illumination under two oxidant conditions: (1) via reaction with  $^3\text{C}^*$  formed from  $5\ \mu\text{mol L}^{-1}$  3,4-dimethoxybenzaldehyde (3,4-DMB) and (2) via reaction with  $\cdot\text{OH}$  generated from  $100\ \mu\text{mol L}^{-1}$  hydrogen peroxide (HOOH; Table 1). Details of the experiments are given in Smith et al. (2014) and a brief summary is given here. Initial solutions were composed of air-saturated Milli-Q water (resistance > 18 M $\Omega$  cm; Millipore) containing

## SOA from aqueous reactions of phenols with two oxidants

L. Yu et al.

Title Page

Abstract

Introduction

Conclusions

References

Tables

Figures



Back

Close

Full Screen / Esc

Printer-friendly Version

Interactive Discussion







## 2.2.2 Nanospray Desorption Electrospray Ionization Mass Spectrometry (nano-DESI MS) measurement and data analysis

Prior to nano-DESI MS analysis, the blown-down samples of phenolic aqSOA were dissolved in Milli-Q water, atomized, and collected on Teflon membrane filters. The analyses were performed using a high-resolution LTQ-Orbitrap mass spectrometer (Thermo Electron, Bremen, Germany) with a resolving power ( $m/\Delta m$ ) of 100 000 at  $m/z = 400$ . The instrument is equipped with a nano-DESI source assembled from two fused-silica capillaries (150  $\mu\text{m}$  o.d./50  $\mu\text{m}$  i.d.) (Roach et al., 2010b). Analyte molecules extracted into the liquid bridge formed between the two capillaries are transferred to a mass spectrometer inlet and ionized by nanoelectrospray. The analysis was performed under the following conditions: spray voltage of 3–5 kV, 0.5–1 mm distance from the tip of the nanospray capillary to the 300 °C heated inlet of the LTQ-Orbitrap, and 0.3–0.9  $\mu\text{L min}^{-1}$  flow rate of acetonitrile : water (1 : 1 volume) solvent. The instrument was calibrated using a standard mixture of caffeine, MRFA (met-arg-phe-ala) peptide, and Ultramark 1621 (Thermo Scientific, Inc.) for the positive ion mode and a standard mixture containing sodium dodecyl sulfate, sodium taurocholate, and Ultramark 1621 (Thermo Scientific, Inc.) for the negative ion mode. Both positive and negative mode mass spectra were acquired using the Xcalibur software (Thermo Electron, Inc.). To analyze a sample, the nano-DESI probe was first placed on a clean area of the filter to record the background signal for  $\sim 3$  min and then positioned on the sample region to acquire data for an additional 4–5 min (Roach et al., 2010a).

Peaks with  $S/N > 10$  were selected using the Decon2LS software developed at the Pacific Northwest National Laboratory (PNNL) (Jaitley et al., 2009). Further data processing was performed with Microsoft Excel using a set of built-in macros developed by Roach et al. (2011). The background and sample peaks were aligned, and the peaks corresponding to  $^{13}\text{C}$  isotopes were removed. Only peaks in the sample spectra that are at least 10 times bigger than the corresponding peaks in the background spectra were retained for further analysis. Peaks were segregated into

ACPD

14, 21149–21187, 2014

### SOA from aqueous reactions of phenols with two oxidants

L. Yu et al.

Title Page

Abstract

Introduction

Conclusions

References

Tables

Figures



Back

Close

Full Screen / Esc

Printer-friendly Version

Interactive Discussion







## SOA from aqueous reactions of phenols with two oxidants

L. Yu et al.

Title Page

Abstract

Introduction

Conclusions

References

Tables

Figures



Back

Close

Full Screen / Esc

Printer-friendly Version

Interactive Discussion



5 a Metrosep RP2 guard/3.6 column and a Metrosep A Supp15 250/4.0 column, and a conductivity detector. Details on the IC method are given in Ge et al. (2014). Briefly, anions were eluted at  $0.8 \text{ mL min}^{-1}$  using an eluent of  $5 \mu\text{mol L}^{-1} \text{ Na}_2\text{CO}_3$  and  $0.3 \mu\text{mol L}^{-1} \text{ NaOH}$  in water. This method can separate and quantify 9 organic anions (glycolate, formate, acetate, pyruvate, oxalate, malate, malonate, maleate, and fumarate) and 7 inorganic anions ( $\text{F}^-$ ,  $\text{Cl}^-$ ,  $\text{NO}_2^-$ ,  $\text{Br}^-$ ,  $\text{NO}_3^-$ ,  $\text{SO}_4^{2-}$  and  $\text{PO}_4^{3-}$ ). The IC results were evaluated in terms of reproducibilities of retention times and peak heights and linearity of the calibration curves. Analysis of external check standards, including a 7-anion standard mixture (Dionex) and 4 individual standards (Metrohm), always produced results that were within 10 % of certified values. Relative differences for replicate analyses were within 3 %.

10 A Shimadzu TOC-VCPH analyzer was applied to measure TOC in the aqSOA samples. The instrument uses a combustion tube filled with oxidation catalyst to convert all carbon atoms into  $\text{CO}_2$  at  $720^\circ\text{C}$  under ultrapure air and quantifies the resulting  $\text{CO}_2$  using a non-dispersive infrared (NDIR) analyzer. Prior to combustion, inorganic carbon species (carbonates/bicarbonates and dissolved  $\text{CO}_2$ ) is transformed into  $\text{CO}_2$  by 25 %  $\text{H}_3\text{PO}_4$ , bubbled out, and determined by NDIR. TOC is determined as the difference. The TOC analyzer was calibrated using the standard solutions of  $\text{NaHCO}_3$ ,  $\text{Na}_2\text{CO}_3$ , and potassium hydrogen phthalate (Sigma-Aldrich or Wako-Japan,  $\geq 99.0\%$ ). Results from external TOC check standards (Aqua Solutions) were always within 10 % of certified values.

### 3 Results and discussion

#### 3.1 Overview of the chemical characteristics of phenolic aqSOA

25 The lifetime of phenols with respect to  $^3\text{C}^*$  and  $\cdot\text{OH}$  reactions in atmospheric fog and cloud water is on the order of minutes to hours during daytime (Smith et al., 2014). Compared to  $\cdot\text{OH}$ , the reaction rates of  $^3\text{C}^*$  with phenols are faster, but the mass yields

**SOA from aqueous reactions of phenols with two oxidants**

L. Yu et al.

Title Page

Abstract

Introduction

Conclusions

References

Tables

Figures



Back

Close

Full Screen / Esc

Printer-friendly Version

Interactive Discussion



of aqSOA from both reactions are near 100 % for phenol, guaiacol, and syringol (Smith et al., 2014). As shown in Fig. 1 and summarized in Table 1, the aqSOA formed from all three phenols with both oxidants are highly oxygenated with average O/C ratios in the range of 0.85–1.23. These results are consistent with a previous study by Sun et al. (2010), where O/C ratios of phenolic aqSOA formed from direct photodegradation and  $\cdot\text{OH}$  oxidation were in the range of 0.80–1.06. The O/C of phenolic SOA from gas-phase  $\cdot\text{OH}$  oxidation are also near unity (Chhabra et al., 2011; Yee et al., 2013). Due to high oxygen contents, the organic mass-to-carbon (OM/OC) ratios of the aqSOA are high (average = 2.27–2.79; Table 1). Note that the OM/OC ratios determined by AMS agree well with those determined based on aqSOA mass measured gravimetrically and organic carbon mass measured by a TOC analyzer (Supplement Fig. S2). For the same oxidant, the O/C ratio of the aqSOA formed at  $t_{1/2}$  follows the order: phenol > guaiacol > syringol (Table 1). This trend is likely driven by precursor reactivity, which determines how long the solution needed to be illuminated to reach one half-life, and has the order: syringol > guaiacol > phenol. Longer illumination time increases the formation of highly oxygenated species and smaller ring-opening species. For the same reason,  $\cdot\text{OH}$  oxidation, which is slower than  $^3\text{C}^*$  reaction for the same phenol precursor, generally produces more oxidized aqSOA at  $t_{1/2}$ .

Figures S3 and S4 in the Supplement show the nano-DESI MS spectra of the aqSOA of syringol, guaiacol, and phenol formed from  $^3\text{C}^*$  and  $\cdot\text{OH}$  reactions, respectively. Hundreds of species were identified, all of which are oxygenated with the median O/C ratios of the molecules varying from 0.33–0.55 in different aqSOA samples (Fig. 1). The signal-weighted average O/C ratios (Bateman et al., 2012) of phenolic aqSOA are in the range of 0.31–0.65 according to the negative ion mode nano-DESI results, which are significantly lower than the average O/C of bulk aqSOA measured by the AMS (Fig. 1). This discrepancy may be attributed to lower electrospray ionization efficiencies of some highly oxidized species or the dissociation of quasi-molecular ions which leads to the loss of highly oxygenated moieties (e.g., loss of  $\text{CO}_2$  for aromatic carboxylic acids) in nano-DESI analysis (Levsen et al., 2007). In addition, in order to provide better

coverage of high-mass ions, nano-DESI mass spectra were analyzed only for ions with  $m/z > 100$ . Therefore, high O/C species with molecular weight lower than 100 dalton (Da), such as oxalate (O/C = 2), formate (O/C = 1), and pyruvate (O/C = 1), were not observed in our nano-DESI experiments. According to IC analysis, these small organic anions together represent 0.8–3.8% of the TOC of aqSOA (Table 1).

Figure 2 shows the AMS spectra of different aqSOA acquired after 50% of the initial phenols had reacted (i.e., at  $t_{1/2}$ ). A prominent feature of these spectra is that  $\text{CO}_2^+$  ( $m/z = 44$ ),  $\text{H}_2\text{O}^+$  ( $m/z = 18$ ), and  $\text{CO}^+$  ( $m/z = 28$ ) are the largest peaks, similar to the spectral pattern of fulvic acid – a model compound representative of highly processed and oxidized organic particulate matter and humic-like substances (HULIS) (Zhang et al., 2005; Ofner et al., 2011). The AMS spectra of syringol aqSOA formed from different oxidants are almost identical (Fig. 2), indicating similar chemical compositions. Similarly, nano-DESI analysis shows the formation of a large number of common species, i.e., 883 species with common elemental composition (Table 1), through the reactions of syringol with  $^3\text{C}^*$  and  $\cdot\text{OH}$ , which account for 76 and 88%, respectively, of the total number of molecules identified in the corresponding aqSOA. A similar overlap of common species was observed for guaiacol aqSOA. But the molecular compositions of phenol aqSOA are more different between the two oxidants (Table 1), which is consistent with the fact that the AMS spectra of the two phenol aqSOA are largely different at  $m/z \geq 80$  (Fig. 2I). The more distinct compositional differences of phenol aqSOA between the  $\cdot\text{OH}$  and  $^3\text{C}^*$  reactions is probably due to the larger difference in reaction times (i.e.,  $t_{1/2} = 672$  min vs. 480 min; Table 1). Detailed discussions on the comparisons of aqSOA produced from the same precursor but different oxidants are given in Sect. 3.3.

A total number of 149 common molecules were identified in all samples (Table 1). Figure 3 shows the Van Krevelen diagram of these common molecules. A majority of these molecules have molecular weight lower than 400 Da and DBE < 12 (Fig. 3), indicating that they contain two or less aromatic rings and that they were likely produced from ring-opening reactions. In addition, small carboxylate anions were observed in all

## SOA from aqueous reactions of phenols with two oxidants

L. Yu et al.

Title Page

Abstract

Introduction

Conclusions

References

Tables

Figures



Back

Close

Full Screen / Esc

Printer-friendly Version

Interactive Discussion



## SOA from aqueous reactions of phenols with two oxidants

L. Yu et al.

Title Page

Abstract

Introduction

Conclusions

References

Tables

Figures



Back

Close

Full Screen / Esc

Printer-friendly Version

Interactive Discussion



aqSOA samples, although they represent only a small fraction of the TOC (Table 1). It is interesting to point out that the number of molecules observed by nano-DESI decreases with increasing illumination time across all 3 phenols, suggesting that increased aging simplifies the products to a smaller set (Table 1). However, this trend could also be related to ionization efficiency of different types of phenolic aqSOA. For example, syringol aqSOA has more methoxy groups, thus is easier to get ionized by nano-DESI, compared to phenol aqSOA.

Both flash-frozen (FF) and blown-down (BD) samples were chemically characterized and show almost identical AMS spectra (Supplement Fig. S5). This is a confirmation that the non-volatile components of these two sample types are chemically very similar. Since FF samples contain dissolved volatile species which should have evaporated during nebulization and drying, we estimated the amount of these species by examining the differences in the TOC concentrations between FF and BD samples after correction for the mass of unreacted precursors. Figure 4 shows the contributions of reactants (phenolic precursor and DMB) and products (dissolved volatile species and aqSOA) to the solution TOC after illumination to  $t_{1/2}$ . Dissolved volatile species formed during photolysis represent a small fraction (2.7–6.6%; Table 1) of the total carbon originally present in the reactants, consistent with the high mass yields of phenolic aqSOA reported by Smith et al. (2014).

### 3.2 Insights into aqSOA formation mechanisms

In this section we synthesize the molecular composition and bulk chemistry results and interpret the formation mechanisms of phenolic aqSOA. A notable result is the large number of dimer and higher oligomers (up to hexamer) found in the aqSOA. As shown in Figs. S3 and S4 in the Supplement, the nano-DESI MS spectra of phenolic aqSOA contain clearly distinguished regions corresponding to monomers, dimers, trimers, tetramers, pentamers, and hexamers and their oxidation products. We therefore determine the distributions of phenolic aqSOA species based on the degree of oligomerization by summing signals in each region (Fig. 5). Oligomers and related

derivative species clearly account for a significant fraction (24.2–92.6%) of the total signals in the nano-DESI spectra of all phenolic aqSOA. Substituted monomers and smaller ring-opening species are also present in all aqSOA and they are particularly abundant in that of phenol + ·OH.

Table 2 lists the 10 most abundant compounds identified in the aqSOA of syringol formed through reaction with ·OH or  $^3\text{C}^*$ . Among them 7 are common species, including syringol dimer ( $\text{C}_{16}\text{H}_{18}\text{O}_6$ ), hydroxylated syringol ( $\text{C}_8\text{H}_{10}\text{O}_5$ ), three dimer derivatives ( $\text{C}_{15}\text{H}_{14}\text{O}_6$ ,  $\text{C}_{15}\text{H}_{16}\text{O}_6$  and  $\text{C}_{15}\text{H}_{16}\text{O}_9$ ), and two monomer derivatives ( $\text{C}_{15}\text{H}_{18}\text{O}_7$  and  $\text{C}_{12}\text{H}_{12}\text{O}_7$ ). Guaiacol aqSOA is also dominated by the dimer and related species whereas substituted monomers are more abundant in phenol aqSOA (Fig. 5). The presence of dimers and substituted monomers is also evident in the AMS spectra. As an example, Fig. 6 shows the AMS spectra of phenol aqSOA along with the NIST mass spectra of possible products. The spectra of guaiacol and syringol aqSOA are shown in Supplement Figs. S6 and S7. Note that the AMS spectrum of biphenyl-4,4'-diol – a substituted phenolic compound – is very similar to the NIST mass spectrum (Supplement Fig. S8), indicating the validity of interpreting the AMS spectra of the phenolic aqSOA based on NIST spectra of possible products. The AMS spectra of phenol aqSOA show a prominent peak at  $m/z = 186$  ( $\text{C}_{12}\text{H}_{10}\text{O}_2^+$ ), which is the molecular ion ( $\text{M}^+$ ) of phenol dimer (Fig. 6). Similarly, the molecular ion of guaiacol dimer ( $\text{C}_{14}\text{H}_{14}\text{O}_4^+$ ;  $m/z = 246$ ; Fig. S6 in the Supplement) is also noticeable in the AMS spectra. These results indicate that oligomerization is an important aqueous-phase reaction pathway that leads to the formation of aqSOA from phenols.

Hydroxylation is another important reaction pathway that forms and transforms phenolic aqSOA. As shown in Supplement Fig. S9, the O-based Kendrick diagram of syringol aqSOA clearly indicates the presence of a large number of species with different degrees of hydroxylation. Similarly, AMS analysis reveals the ubiquitous formation of hydroxylated products as well. For example, the AMS spectra of phenol aqSOA show prominent peaks at  $m/z = 110$  ( $\text{C}_6\text{H}_6\text{O}_2^+$ ) and  $m/z = 202$  ( $\text{C}_{12}\text{H}_{10}\text{O}_3^+$ ), suggesting the presence of hydroxylated phenol and hydroxylated phenol dimer, respectively (Fig. 6).

## SOA from aqueous reactions of phenols with two oxidants

L. Yu et al.

[Title Page](#)[Abstract](#)[Introduction](#)[Conclusions](#)[References](#)[Tables](#)[Figures](#)[Back](#)[Close](#)[Full Screen / Esc](#)[Printer-friendly Version](#)[Interactive Discussion](#)

In addition, signature ions representing 2-methoxyhydroquinone are detected in guaiacol aqSOA (Fig. S6 in the Supplement) and 3,4,5-trihydroxy benzoic acid is likely a product of syringol oxidation (Supplement Fig. S7)

Both nano-DESI and AMS results further reveal the broad formation of aldehydes, esters, and carboxylated products. As shown in Table 2,  $C_9H_{10}O_4$  (MW = 182; DBE = 5), which was found to present at high abundance in the aqSOA of syringol +  $^3C^*$ , is likely a syringol aldehyde. In addition, the pronounced  $C_7H_5O_2^+$  ( $m/z = 121$ ) peak in the AMS spectra of phenol aqSOA (Fig. 6a) indicates the formation of phenol esters such as methylparaben and ethylparaben (Fig. 6d) and the prominent  $C_8H_7O_3^+$  ( $m/z = 151$ ) signal in the guaiacol aqSOA spectra (Fig. S6a in the Supplement) suggests the formation of a guaiacol ester – methyl vanillate (Supplement Fig. S6c).

Small organic acid anions (i.e., formate, acetate, oxalate, malate, malonate, etc.) are observed in all samples and these species together account for less than 4% of the TOC in aqSOA (Table 1). Note that the importance of organic acids is likely underestimated as IC only quantifies a limited number of low molecular weight aliphatic acids. Nano-DESI analysis further reveals the presence of a number of aromatic compounds with substituted carboxyl groups (e.g., aromatic esters; Supplement Fig. S10) and the formation of highly oxygenated C3–C5 aliphatic species in all samples, some of which (e.g.,  $C_3H_4O_4$ ,  $C_4H_6O_4$  and  $C_5H_6O_5$ ) are likely carboxylic acids based on DBE values. Furthermore, both nano-DESI and AMS analyses identify demethoxylated aromatic products (e.g.,  $C_{15}H_{16}O_6$  and  $C_{15}H_{16}O_9$  in Table 2). These results together indicate that various fragmentation pathways, such as the cleavage of the aromatic rings and the losses of methoxy ( $-OCH_3$ ) groups, are also important during the aqueous-phase reactions of phenols.

Based on these results, we propose a scheme in Fig. 7 of the main pathways of aqSOA formation through the reactions of phenols +  $^3C^*$ . Briefly, phenols react with  $^3C^*$  and undergo multiple steps to eventually form HOOH (Anastasio et al., 1997), which is a source of  $\cdot OH$  via photolysis. The addition of  $\cdot OH$  to the aromatic ring, followed by  $O_2$  addition and  $HO_2$  elimination, lead to the formation of hydroxylated products (Barzaghi

## SOA from aqueous reactions of phenols with two oxidants

L. Yu et al.

Title Page

Abstract

Introduction

Conclusions

References

Tables

Figures



Back

Close

Full Screen / Esc

Printer-friendly Version

Interactive Discussion



and Herrmann, 2002). In the meantime, the ·OH-phenol adduct can undergo unimolecular elimination of H<sub>2</sub>O to form a phenoxy radical (Atkinson et al., 1992; Barzaghi and Herrmann, 2002; Olariu et al., 2002), which then combines with another radical to form dimer and higher oligomers. Phenoxy radical may also form from the oxidation of phenols by <sup>3</sup>C\* via electron transfer coupled with proton transfer from the phenoxy radical cation or from solvent water (Anastasio et al., 1997). Demethoxylation takes place through attachment of ·OH to ring positions occupied by methoxyl groups, followed by elimination of a methanol molecule to form semiquinone radicals (Steenken and O'Neill, 1977). Esterification of phenols can occur as a result of the reactions with organic acids (Offenhauer, 1964). Furthermore, the reactants and the products from all these pathways may undergo ring-opening process, forming ketones and carboxylic acids. Similar species, including oligomers, esters, carbonyls, carboxylic acids, and demethoxylated products, can be formed in ·OH-mediated reactions as well (Sun et al., 2010), although apparently with different reaction yields and rates.

### 3.3 Comparisons of phenolic aqSOA produced from different oxidants: ·OH vs. <sup>3</sup>C\*

As discussed above, aqueous reactions of phenols produce a variety of low-volatility species including oligomers, functionalized monomer and oligomers (with varying numbers of carbonyl, carboxyl, ester, and hydroxyl groups), and small organic acids (e.g., formate, acetate, oxalate, and malate). Although aqSOA formed from the same precursor generally appear to be chemically similar, there are significant compositional differences between the products from ·OH and <sup>3</sup>C\* reactions. Overall, the molecular compositions of guaiacol and phenol aqSOA are more dependent on the oxidant than are syringol aqSOA (Fig. 5). Similarly, the AMS spectral patterns at *m/z* ≥ 80 exhibit more significant differences between ·OH and <sup>3</sup>C\* for guaiacol (*r*<sup>2</sup> = 0.65; Fig. 2j) and phenol (*r*<sup>2</sup> = 0.42; Fig. 2l) whereas those for syringol are almost identical (*r*<sup>2</sup> = 0.97; Fig. 2h). Furthermore, a majority of the aqSOA molecules of phenol + ·OH contain only

## SOA from aqueous reactions of phenols with two oxidants

L. Yu et al.

Title Page

Abstract

Introduction

Conclusions

References

Tables

Figures



Back

Close

Full Screen / Esc

Printer-friendly Version

Interactive Discussion



one benzene ring, whereas the  $^3\text{C}^*$  reaction produces more oligomers and substituted species based on the DBE values.

Since the AMS results are quantitative, we further compare the relative abundances of signature ions in the AMS spectra of different aqSOA (Fig. 8). Details on the signature ions and their proposed precursors are given in Supplement Table S1. All these ions are odd electron ions, which usually have special mechanistic significances and are more indicative of the chemical identities of the precursors (McLafferty and Turecek, 1993). These ions can potentially be used to analyze ambient organic aerosol data for the presence of phenolic aqSOA. For instance, a previous study by our group observed  $\text{C}_{16}\text{H}_{18}\text{O}_6^+$  ( $m/z$  306) and  $\text{C}_{14}\text{H}_{14}\text{O}_4^+$  ( $m/z$  246) – signature ions representing syringol and guaiacol dimers, respectively, in ambient aerosols significantly influenced by wood combustion and fog processing (Sun et al., 2010). Similar to the nano-DESI results, the AMS results also indicate that the aqSOA formed via  $^3\text{C}^*$  are more enriched of dimers and higher oligomers compared to  $\cdot\text{OH}$  for a given phenol. These observations suggest that more coupling of phenoxy radicals takes place during reactions initiated by  $^3\text{C}^*$  than by  $\cdot\text{OH}$ . On the other hand, both IC and nano-DESI results indicate that  $\cdot\text{OH}$ -mediated reactions promote the formation of organic acids and other small ring-opening species (see Sect. 3.2), consistent with the observations that  $\cdot\text{OH}$  reaction generally leads to more oxidized aqSOA as well as water-soluble volatile species (Table 1).

A possible reason for the compositional differences observed in the aqSOA of the same precursor but different oxidants is that  $^3\text{C}^*$  reacts faster with phenols (Smith et al., 2014) and thus takes shorter time to oxidize the same amount of phenols compared to  $\cdot\text{OH}$ . Longer illumination allows further oxidation and fragmentation of higher molecular weight species to happen, leading to the formation of smaller molecules with fewer aromatic rings. Indeed, the compositions of syringol aqSOA, which were produced after comparable illumination durations, are highly similar between the two oxidation conditions according to both nano-DESI and AMS results whereas the difference is the largest for phenol aqSOA whose illumination times are substantially different between

## SOA from aqueous reactions of phenols with two oxidants

L. Yu et al.

Title Page

Abstract

Introduction

Conclusions

References

Tables

Figures



Back

Close

Full Screen / Esc

Printer-friendly Version

Interactive Discussion





$^3\text{C}^*$  and  $\cdot\text{OH}$  oxidation (Figs. 2 and 5). However, the fact that there are more oligomers and their derivatives in guaiacol +  $^3\text{C}^*$  condition compared to syringol +  $\cdot\text{OH}$  (Fig. 5) even though the guaiacol solution was illuminated longer (Table 1) suggests that coupling of phenoxy radicals is a more favored pathway through  $^3\text{C}^*$  reaction.

### 3.4 Volatility profiles and UV-vis absorption spectra of phenolic aqSOA

As discussed above, the chemical compositions of the phenolic aqSOA are complex. As a result, the volatilities of the aqSOA species span a broad range, from very low vapor pressure compounds such as oligomers to more volatile species such as low molecular weight acids. Figure 9 shows the volatility profiles of phenolic aqSOA formed from  $^3\text{C}^*$  reactions measured by a thermodenuder coupled with the AMS. Ammonium sulfate and ammonium nitrate were analyzed simultaneously as references. On average, phenolic aqSOA are more volatile than ammonium sulfate, but less volatile than ammonium nitrate (Fig. 9). The fact that a significant fraction of the aqSOA mass remains in the particle phase even at 200 °C (Fig. 9) is consistent with the presence of some very low volatility species such as oligomers. Compared to guaiacol and syringol aqSOA, phenol aqSOA show the slowest decay with increasing TD temperature, indicating that they are comprised of more low-volatility species. This is consistent with our chemical analyses which reveal that the aqSOA of phenol +  $^3\text{C}^*$  are composed of a larger fraction of species containing more than two aromatic rings, including trimer and higher oligomers (Fig. 5) and that the O/C ratios of phenol aqSOA are also highest among all for the same oxidant. These results together suggest that the volatility of phenolic aqSOA is strongly influenced by both polymer contents and average oxidation degree, as reported previously (Huffman et al., 2009).

Recently, light-absorbing OA, also termed as “brown carbon”, has attracted much attention, due to their ability to absorb sunlight thus affect the radiative budget of the earth (Shapiro et al., 2009). Previous studies have shown that the aqueous-phase oxidation of phenols forms low-volatility oligomers, which absorb significant amounts

## SOA from aqueous reactions of phenols with two oxidants

L. Yu et al.

Title Page

Abstract

Introduction

Conclusions

References

Tables

Figures



Back

Close

Full Screen / Esc

Printer-friendly Version

Interactive Discussion



of UV-visible light and likely account for a significant portion of atmospheric HULIS (Gelencser et al., 2003; Chang and Thompson, 2010). In this study, we examined the optical properties of phenolic aqSOA using UV-vis spectroscopy. Figure 10 shows an example of the UV-vis spectra of syringol aqSOA formed in the reactions with  $^3\text{C}^*$  and  $\cdot\text{OH}$ , respectively, at  $t_{1/2}$ . Both syringol aqSOA samples absorb in the tropospheric sunlight wavelengths ( $> 300\text{nm}$ ), while syringol does not. This enhancement is likely explained by the formation of conjugated structures as a result of polymerization and functionalization due to the additions of hydroxyl, carbonyl, and carboxyl functional groups to the aromatic rings. These results indicate that aqueous-phase reactions of phenols are likely an important source of brown carbon in the atmosphere, especially in regions influenced by biomass burning.

#### 4 Conclusions and implications

We thoroughly characterized the chemical composition and studied the volatility and optical properties of phenolic aqSOA formed via reactions with two different oxidants:  $^3\text{C}^*$  and  $\cdot\text{OH}$ . Elemental analysis of the AMS spectra indicates that all phenolic aqSOA are highly oxidized (O/C ratios: 0.85–1.23), despite the fact that some of the reactions were very fast ( $t_{1/2} < 1\text{h}$  for syringol). For the same oxidant, the oxidation degree of the aqSOA formed at  $t_{1/2}$  follows the order: phenol  $>$  guaiacol  $>$  syringol. A large number of aqSOA molecules are identified, including oligomers (up to hexamers) and their derivatives with varying numbers of carbonyl, carboxyl, ester, and hydroxyl groups. A large number of ring-opening species including small organic acids (e.g., oxalate, formate, and acetate) are also identified. While the bulk compositions of the aqSOA are overall similar at  $t_{1/2}$  between the two oxidants for a given precursor, compositional differences are observed. Generally speaking, reactions mediated by  $\cdot\text{OH}$  produce more highly oxygenated species with a single aromatic ring, while oxidation by  $^3\text{C}^*$  enhances the formation of higher molecular weight species including oligomers and their oxygenated derivatives. The physical properties, such as volatility and light absorptivity,

## SOA from aqueous reactions of phenols with two oxidants

L. Yu et al.

Title Page

Abstract

Introduction

Conclusions

References

Tables

Figures



Back

Close

Full Screen / Esc

Printer-friendly Version

Interactive Discussion



of the phenol aqSOA depend on their chemical compositions. Our thermodenuder experiments indicate that the volatility profiles of phenolic aqSOA are influenced by both oligomer contents and average oxidation degree. In addition, the formation of aqSOA species with enhanced conjugated double bonds is probably responsible for the significant light absorption in the actinic region, suggesting that aqueous-phase reactions of phenols are an important source of brown carbon in the atmosphere.

Overall, our results indicate that aqueous-phase processing of phenols represents an important pathway for the production of low-volatility, highly oxygenated and high molecular weight species, which remain in the particle phase after water evaporation. Since aqSOA formed from reactions of phenolic compounds are both water soluble and light absorbing, these reactions might significantly influence the chemical and physical properties, and thus the climatic and health effects, of atmospheric particles in regions influenced by biomass burning emissions. In this study, we also identified a number of AMS signature ions that are representative of phenolic aqSOA, e.g.,  $C_{16}H_{18}O_6^+$  ( $m/z = 306$ ) for syringol dimer,  $C_{14}H_{14}O_4^+$  ( $m/z = 246$ ) for guaiacol dimer,  $C_{14}H_{14}O_5^+$  ( $m/z = 262$ ) and  $C_{14}H_{14}O_6^+$  ( $m/z = 278$ ) for hydroxylated guaiacol dimer,  $C_{12}H_{10}O_2^+$  ( $m/z = 186$ ) for phenol dimer,  $C_{21}H_{20}O_6^+$  ( $m/z = 368$ ) for guaiacol trimer, and  $C_{18}H_{14}O_3^+$  ( $m/z = 278$ ) for phenol trimer (Fig. 8). AMS has been broadly applied for chemical analysis of ambient aerosol and multivariate statistical approaches (e.g., positive matrix factorization) have been frequently used on organic aerosol mass spectral data to determine factors representing different sources and processes (Ulbrich et al., 2009; Zhang et al., 2011). An important criterion for validating the extracted factor is via examining the mass spectra of the factors for signature ions (Zhang et al., 2011). The signature ions identified in this study could be compared to ambient organic aerosol mass spectrometry data to investigate the impacts of phenolic aqSOA formation.

The Supplement related to this article is available online at  
doi:10.5194/acpd-14-21149-2014-supplement.

**SOA from aqueous reactions of phenols with two oxidants**

L. Yu et al.

Title Page

Abstract

Introduction

Conclusions

References

Tables

Figures



Back

Close

Full Screen / Esc

Printer-friendly Version

Interactive Discussion



*Acknowledgement.* This work was supported by the US National Science Foundation, Grant No. AGS-1036675, the California Agricultural Experiment Station (Projects CA-D-ETX-2102-H and CA-D\*-LAW-6403-RR). The nano-DESI measurements were performed at the W. R. Wiley Environmental Molecular Sciences Laboratory (EMSL) – a national scientific user facility located at PNNL, and sponsored by the Office of Biological and Environmental Research of the US PNNL is operated for US DOE by Battelle Memorial Institute under contract no. DE-AC06-76RL0 1830. Additional funding was provided by a Jastro-Shields Graduate Research Award (UC Davis) and a graduate fellowship from the Atmospheric Aerosols and Health (AAH) program at UC Davis to L. Yu. We thank A. Dillner, K. George, and S. Collier for help with experiments.

**References**

- Aiken, A. C., DeCarlo, P. F., Kroll, J. H., Worsnop, D. R., Huffman, J. A., Canagaratna, M. R., Onasch, T. B., Alfarra, M. R., Prevot, A. S. H., Dommen, J., Duplissy, J., Metzger, A., Baltensperger, U., and Jimenez, J. L.: O/C and OM/OC ratios of primary, secondary, and ambient organic aerosols with a high resolution time-of-flight aerosol mass spectrometer, *Environ. Sci. Technol.*, 42, 4478–4485, doi:10.1021/es703009q, 2008.
- Allan, J. D., Delia, A. E., Coe, H., Bower, K. N., Alfarra, M. R., Jimenez, J. L., Middlebrook, A. M., Drewnick, F., Onasch, T. B., Canagaratna, M. R., Jayne, J. T., and Worsnop, D. R.: A generalised method for the extraction of chemically resolved mass spectra from Aerodyne aerosol mass spectrometer data, *J. Aerosol Sci.*, 35, 909–922, doi:10.1016/j.jaerosci.2004.02.007, 2004.
- Altieri, K. E., Carlton, A. G., Lim, H. J., Turpin, B. J., and Seitzinger, S. P.: Evidence for oligomer formation in clouds: reactions of isoprene oxidation products, *Environ. Sci. Technol.*, 40, 4956–4960, doi:10.1021/es052170n, 2006.
- Anastasio, C., Faust, B. C., and Rao, C. J.: Aromatic carbonyl compounds as aqueous-phase photochemical sources of hydrogen peroxide in acidic sulfate aerosols, fogs, and clouds .1. non-phenolic methoxybenzaldehydes and methoxyacetophenones with reductants (phenols), *Environ. Sci. Technol.*, 31, 218–232, doi:10.1021/es960359g, 1997.

## SOA from aqueous reactions of phenols with two oxidants

L. Yu et al.

Title Page

Abstract

Introduction

Conclusions

References

Tables

Figures



Back

Close

Full Screen / Esc

Printer-friendly Version

Interactive Discussion



Atkinson, R., Aschmann, S. M., and Arey, J.: Reactions of hydroxyl and nitrogen trioxide radicals with phenol, cresols, and 2-nitrophenol at  $296 \pm 2$  K, *Environ. Sci. Technol.*, 26, 1397–1403, doi:10.1021/es00031a018, 1992.

Barzaghi, P. and Herrmann, H.: A mechanistic study of the oxidation of phenol by OH/NO<sub>2</sub>/NO<sub>3</sub> in aqueous solution, *Phys. Chem. Chem. Phys.*, 4, 3669–3675, doi:10.1039/b201652d, 2002.

Bateman, A. P., Laskin, J., Laskin, A., and Nizkorodov, S. A.: Applications of high-resolution electrospray ionization mass spectrometry to measurements of average oxygen to carbon ratios in secondary organic aerosols, *Environ. Sci. Technol.*, 46, 8315–8324, doi:10.1021/es3017254, 2012.

Blando, J. D. and Turpin, B. J.: Secondary organic aerosol formation in cloud and fog droplets: a literature evaluation of plausibility, *Atmos. Environ.*, 34, 1623–1632, doi:10.1016/S1352-2310(99)00392-1, 2000.

Canagaratna, M., Jayne, J., Jimenez, J. L., Allan, J. A., Alfarra, R., Zhang, Q., Onasch, T., Drewnick, F., Coe, H., Middlebrook, A., Delia, A., Williams, L., Trimborn, A., Northway, M., DeCarlo, P., Kolb, C., Davidovits, P., and Worsnop, D.: Chemical and microphysical characterization of ambient aerosols with the aerodyne aerosol mass spectrometer, *Mass Spectrom. Rev.*, 26, 185–222, doi:10.1002/mas.20115, 2007.

Canonica, S., Hellrung, B., and Wirz, J.: Oxidation of phenols by triplet aromatic ketones in aqueous solution, *J. Phys. Chem. A*, 104, 1226–1232, doi:10.1021/jp9930550, 2000.

Chang, J. L. and Thompson, J. E.: Characterization of colored products formed during irradiation of aqueous solutions containing H<sub>2</sub>O<sub>2</sub> and phenolic compounds, *Atmos. Environ.*, 44, 541–551, doi:10.1016/j.atmosenv.2009.10.042, 2010.

Chhabra, P. S., Ng, N. L., Canagaratna, M. R., Corrigan, A. L., Russell, L. M., Worsnop, D. R., Flagan, R. C., and Seinfeld, J. H.: Elemental composition and oxidation of chamber organic aerosol, *Atmos. Chem. Phys.*, 11, 8827–8845, doi:10.5194/acp-11-8827-2011, 2011.

Collier, S. and Zhang, Q.: Gas-phase CO<sub>2</sub> subtraction for improved measurements of the organic aerosol mass concentration and oxidation degree by an aerosol mass spectrometer, *Environ. Sci. Technol.*, 47, 14324–14331, doi:10.1021/es404024h, 2013.

DeCarlo, P. F., Kimmel, J. R., Trimborn, A., Northway, M. J., Jayne, J. T., Aiken, A. C., Gonin, M., Fuhrer, K., Horvath, T., Docherty, K. S., Worsnop, D. R., and Jimenez, J. L.: Field-deployable, high-resolution, time-of-flight aerosol mass spectrometer, *Anal. Chem.*, 78, 8281–8289, doi:10.1021/ac061249n, 2006.

**SOA from aqueous reactions of phenols with two oxidants**

L. Yu et al.

Title Page

Abstract

Introduction

Conclusions

References

Tables

Figures



Back

Close

Full Screen / Esc

Printer-friendly Version

Interactive Discussion



- Ervens, B., Turpin, B. J., and Weber, R. J.: Secondary organic aerosol formation in cloud droplets and aqueous particles (aqSOA): a review of laboratory, field and model studies, *Atmos. Chem. Phys.*, 11, 11069–11102, doi:10.5194/acp-11-11069-2011, 2011.
- Fierz, M., Vernooij, M. G. C., and Burtscher, H.: An improved low-flow thermodenuder, *J. Aerosol Sci.*, 38, 1163–1168, doi:10.1016/j.jaerosci.2007.08.006, 2007.
- Ge, X., Shaw, S. L., and Zhang, Q.: Toward understanding amines and their degradation products from postcombustion CO<sub>2</sub> capture processes with aerosol mass spectrometry, *Environ. Sci. Technol.*, 48, 5066–5075, doi:10.1021/es4056966, 2014.
- Gelencser, A., Hoffer, A., Kiss, G., Tombacz, E., Kurdi, R., and Bencze, L.: In-situ formation of light-absorbing organic matter in cloud water, *J. Atmos. Chem.*, 45, 25–33, doi:10.1023/a:1024060428172, 2003.
- George, K. M., Ruthenburg, T. C., Smith, J. D., Anastasio, C., Yu, L., Zhang, Q., and Dillner, A.: FT-IR quantification of the carbonyl functional group in aqueous-phase secondary organic aerosol from phenols, *Atmos. Environ.*, submitted, 2014.
- Hallquist, M., Wenger, J. C., Baltensperger, U., Rudich, Y., Simpson, D., Claeys, M., Dommen, J., Donahue, N. M., George, C., Goldstein, A. H., Hamilton, J. F., Herrmann, H., Hoffmann, T., Iinuma, Y., Jang, M., Jenkin, M. E., Jimenez, J. L., Kiendler-Scharr, A., Maenhaut, W., McFiggans, G., Mentel, Th. F., Monod, A., Prévôt, A. S. H., Seinfeld, J. H., Surratt, J. D., Szmigielski, R., and Wildt, J.: The formation, properties and impact of secondary organic aerosol: current and emerging issues, *Atmos. Chem. Phys.*, 9, 5155–5236, doi:10.5194/acp-9-5155-2009, 2009.
- Hawthorne, S. B., Krieger, M. S., Miller, D. J., and Mathiason, M. B.: Collection and quantitation of methoxylated phenol tracers for atmospheric-pollution from residential wood stoves, *Environ. Sci. Technol.*, 23, 470–475, doi:10.1021/es00181a013, 1989.
- Hawthorne, S. B., Miller, D. J., Langenfeld, J. J., and Krieger, M. S.: PM-10 high-volume collection and quantitation of semi- and nonvolatile phenols, methoxylated phenols, alkanes, and polycyclic aromatic hydrocarbons from winter urban air and their relationship to wood smoke emissions, *Environ. Sci. Technol.*, 26, 2251–2262, doi:10.1021/es00035a026, 1992.
- Huffman, J. A., Docherty, K. S., Mohr, C., Cubison, M. J., Ulbrich, I. M., Ziemann, P. J., Onasch, T. B., and Jimenez, J. L.: Chemically-resolved volatility measurements of organic aerosol from different sources, *Environ. Sci. Technol.*, 43, 5351–5357, doi:10.1021/es803539d, 2009.

**SOA from aqueous reactions of phenols with two oxidants**

L. Yu et al.

[Title Page](#)[Abstract](#)[Introduction](#)[Conclusions](#)[References](#)[Tables](#)[Figures](#)[Back](#)[Close](#)[Full Screen / Esc](#)[Printer-friendly Version](#)[Interactive Discussion](#)

Hughey, C. A., Hendrickson, C. L., Rodgers, R. P., Marshall, A. G., and Qian, K. N.: Kendrick mass defect spectrum: a compact visual analysis for ultrahigh-resolution broadband mass spectra, *Anal. Chem.*, 73, 4676–4681, doi:10.1021/ac010560w, 2001.

Jaitly, N., Mayampurath, A., Littlefield, K., Adkins, J. N., Anderson, G. A., and Smith, R. D.: Decon2LS: An open-source software package for automated processing and visualization of high resolution mass spectrometry data, *BMC Bioinformatics*, 10, 87, doi:10.1186/1471-2105-10-87, 2009.

Jimenez, J. L., Canagaratna, M. R., Donahue, N. M., Prevot, A. S. H., Zhang, Q., Kroll, J. H., DeCarlo, P. F., Allan, J. D., Coe, H., Ng, N. L., Aiken, A. C., Docherty, K. D., Ulbrich, I. M., Grieshop, A. P., Duplissy, A. L. R. J., Smith, J. D., Wilson, K. R., Lanz, V. A., Hueglin, C., Sun, Y. L., Tian, J., Laaksonen, A., Raatikainen, T., Rautiainen, J., Vaattovaara, P., Ehn, M., Kulmala, M., Tomlinson, J. M., Collins, D. R., Cubison, M. J., Dunlea, E. J., Huffman, J. A., Onasch, T. B., Alfarra, M. R., Williams, P. I., Bower, K., Kondo, Y., Schneider, J., Drewnick, F., Borrmann, S., Weimer, S., Demerjian, K., Salcedo, D., Cottrell, L., Griffin, R., Takami, A., Hatakeyama, T. M. S., Shimono, A., Zhang, J. Y. S. Y. M., Kimmel, K. D. J. R., Sueper, D., Jayne, J. T., Herndon, S. C., Trimborn, A. M., Williams, L. R., Wood, E. C., Kolb, C. E., Baltensperger, U., and Worsnop, D. R.: Evolution of organic aerosols in the atmosphere, *Science*, 326, 1525–1529, doi:10.1126/science.1180353, 2009.

Kanakidou, M., Seinfeld, J. H., Pandis, S. N., Barnes, I., Dentener, F. J., Facchini, M. C., Van Dingenen, R., Ervens, B., Nenes, A., Nielsen, C. J., Swietlicki, E., Putaud, J. P., Balkanski, Y., Fuzzi, S., Horth, J., Moortgat, G. K., Winterhalter, R., Myhre, C. E. L., Tsigaridis, K., Vignati, E., Stephanou, E. G., and Wilson, J.: Organic aerosol and global climate modelling: a review, *Atmos. Chem. Phys.*, 5, 1053–1123, doi:10.5194/acp-5-1053-2005, 2005.

Leuenerger, C., Ligocki, M. P., and Pankow, J. F.: Trace organic compounds in rain. 4. Identities, concentrations, and scavenging mechanisms for phenols in urban air and rain, *Environ. Sci. Technol.*, 19, 1053–1058, doi:10.1021/es00141a005, 1985.

Levsen, K., Schiebel, H. M., Terlouw, J. K., Jobst, K. J., Elend, M., Preiss, A., Thiele, H., and Ingendoh, A.: Even-electron ions: a systematic study of the neutral species lost in the dissociation of quasi-molecular ions, *J. Mass Spectrom.*, 42, 1024–1044, doi:10.1002/jms.1234, 2007.

Lim, H. J., Carlton, A. G., and Turpin, B. J.: Isoprene forms secondary organic aerosol through cloud processing: model simulations, *Environ. Sci. Technol.*, 39, 4441–4446, doi:10.1021/es048039h, 2005.

**SOA from aqueous reactions of phenols with two oxidants**

L. Yu et al.

Title Page

Abstract

Introduction

Conclusions

References

Tables

Figures



Back

Close

Full Screen / Esc

Printer-friendly Version

Interactive Discussion



- McLafferty, F. W. and Turecek, F.: Interpretation of Mass Spectra, University Science Books, Mill Valley, California, 1993.
- Murphy, D. M., Cziczo, D. J., Froyd, K. D., Hudson, P. K., Matthew, B. M., Middlebrook, A. M., Peltier, R. E., Sullivan, A., Thomson, D. S., and Weber, R. J.: Single-particle mass spectrometry of tropospheric aerosol particles, *J. Geophys. Res.-Atmos.*, 111, D23S32, doi:10.1029/2006jd007340, 2006.
- Offenhauer, R. D.: The direct esterification of phenols, *J. Chem. Educ.*, 41, 39, doi:10.1021/ed041p39, 1964.
- Ofner, J., Krüger, H.-U., Grothe, H., Schmitt-Kopplin, P., Whitmore, K., and Zetzsch, C.: Physico-chemical characterization of SOA derived from catechol and guaiacol – a model substance for the aromatic fraction of atmospheric HULIS, *Atmos. Chem. Phys.*, 11, 1–15, doi:10.5194/acp-11-1-2011, 2011.
- Olariu, R. I., Klotz, B., Barnes, I., Becker, K. H., and Mocanu, R.: FT-IR study of the ring-retaining products from the reaction of OH radicals with phenol, *o*-, *m*-, and *p*-cresol, *Atmos. Environ.*, 36, 3685–3697, doi:10.1016/s1352-2310(02)00202-9, 2002.
- Pellegrin, V.: Molecular formulas of organic compounds: the nitrogen rule and degree of unsaturation, *J. Chem. Educ.*, 60, 626–633, doi:10.1021/ed060p626, 1983.
- Roach, P. J., Laskin, J., and Laskin, A.: Molecular characterization of organic aerosols using nanospray-desorption/electrospray ionization-mass spectrometry, *Anal. Chem.*, 82, 7979–7986, doi:10.1021/ac101449p, 2010a.
- Roach, P. J., Laskin, J., and Laskin, A.: Nanospray desorption electrospray ionization: an ambient method for liquid-extraction surface sampling in mass spectrometry, *Analyst*, 135, 2233–2236, doi:10.1039/c0an00312c, 2010b.
- Roach, P. J., Laskin, J., and Laskin, A.: Higher-order mass defect analysis for mass spectra of complex organic mixtures, *Anal. Chem.*, 83, 4924–4929, doi:10.1021/ac200654j, 2011.
- Sagebiel, J. C. and Seiber, J. N.: Studies on the occurrence and distribution of wood smoke marker compounds in foggy atmospheres, *Environ. Toxicol. Chem.*, 12, 813–822, doi:10.1002/etc.5620120504, 1993.
- Sander, R.: Compilation of Henry's Law constants for inorganic and organic species of potential importance in environmental chemistry, available at: <http://irs.ub.rug.nl/dbi/4581696d8b3ed> (last access: 14 December 2006), 1999.



**SOA from aqueous reactions of phenols with two oxidants**

L. Yu et al.

Title Page

Abstract

Introduction

Conclusions

References

Tables

Figures



Back

Close

Full Screen / Esc

Printer-friendly Version

Interactive Discussion



Schauer, J. J., Kleeman, M. J., Cass, G. R., and Simoneit, B. R. T.: Measurement of emissions from air pollution sources. 3. C-1-C-29 organic compounds from fireplace combustion of wood, *Environ. Sci. Technol.*, 35, 1716–1728, doi:10.1021/es001331e, 2001.

Shapiro, E. L., Szprengiel, J., Sareen, N., Jen, C. N., Giordano, M. R., and McNeill, V. F.: Light-absorbing secondary organic material formed by glyoxal in aqueous aerosol mimics, *Atmos. Chem. Phys.*, 9, 2289–2300, doi:10.5194/acp-9-2289-2009, 2009.

Simoneit, B. R. T., Schauer, J. J., Nolte, C. G., Oros, D. R., Elias, V. O., Fraser, M. P., Rogge, W. F., and Cass, G. R.: Levoglucosan, a tracer for cellulose in biomass burning and atmospheric particles, *Atmos. Environ.*, 33, 173–182, doi:10.1016/s1352-2310(98)00145-9, 1999.

Smith, J. D., Sio, V., Yu, L., Zhang, Q., and Anastasio, C.: Secondary organic aerosol production from aqueous reactions of atmospheric phenols with an organic triplet excited state, *Environ. Sci. Technol.*, 48, 1049–1057, doi:10.1021/es4045715, 2014.

Steenken, S. and O'Neill, P.: Oxidative demethoxylation of methoxylated phenols and hydroxybenzoic acids by the hydroxyl radical. An in situ electron spin resonance, conductometric pulse radiolysis and product analysis study, *J. Phys. Chem.*, 81, 505–508, doi:10.1021/j100521a002, 1977.

Sun, Y., Zhang, Q., Macdonald, A. M., Hayden, K., Li, S. M., Liggio, J., Liu, P. S. K., Anlauf, K. G., Leaitch, W. R., Steffen, A., Cubison, M., Worsnop, D. R., van Donkelaar, A., and Martin, R. V.: Size-resolved aerosol chemistry on Whistler Mountain, Canada with a high-resolution aerosol mass spectrometer during INTEX-B, *Atmos. Chem. Phys.*, 9, 3095–3111, doi:10.5194/acp-9-3095-2009, 2009.

Sun, Y. L., Zhang, Q., Anastasio, C., and Sun, J.: Insights into secondary organic aerosol formed via aqueous-phase reactions of phenolic compounds based on high resolution mass spectrometry, *Atmos. Chem. Phys.*, 10, 4809–4822, doi:10.5194/acp-10-4809-2010, 2010.

Ulbrich, I. M., Canagaratna, M. R., Zhang, Q., Worsnop, D. R., and Jimenez, J. L.: Interpretation of organic components from Positive Matrix Factorization of aerosol mass spectrometric data, *Atmos. Chem. Phys.*, 9, 2891–2918, doi:10.5194/acp-9-2891-2009, 2009.

Yee, L. D., Kautzman, K. E., Loza, C. L., Schilling, K. A., Coggon, M. M., Chhabra, P. S., Chan, M. N., Chan, A. W. H., Hersey, S. P., Crounse, J. D., Wennberg, P. O., Flagan, R. C., and Seinfeld, J. H.: Secondary organic aerosol formation from biomass burning intermediates: phenol and methoxyphenols, *Atmos. Chem. Phys.*, 13, 8019–8043, doi:10.5194/acp-13-8019-2013, 2013.

**SOA from aqueous reactions of phenols with two oxidants**

L. Yu et al.

Title Page

Abstract

Introduction

Conclusions

References

Tables

Figures



Back

Close

Full Screen / Esc

Printer-friendly Version

Interactive Discussion



- Zhang, Q., Alfarra, M. R., Worsnop, D. R., Allan, J. D., Coe, H., Canagaratna, M. R., and Jimenez, J. L.: Deconvolution and quantification of hydrocarbon-like and oxygenated organic aerosols based on aerosol mass spectrometry, *Environ. Sci. Technol.*, 39, 4938–4952, doi:10.1021/es048568l, 2005.
- 5 Zhang, Q., Jimenez, J. L., Canagaratna, M. R., Allan, J. D., Coe, H., Ulbrich, I., Alfarra, M. R., Takami, A., Middlebrook, A. M., Sun, Y. L., Dzepina, K., Dunlea, E., Docherty, K., DeCarlo, P. F., Salcedo, D., Onasch, T., Jayne, J. T., Miyoshi, T., Shimojo, A., Hatakeyama, S., Takegawa, N., Kondo, Y., Schneider, J., Drewnick, F., Weimer, S., Demerjian, K., Williams, P., Bower, K., Bahreini, R., Cotrell, L., Griffin, R. J., Rautiainen, J., Sun, J. Y., Zhang, Y. M., and Worsnop, D. R.: Ubiquity and dominance of oxygenated species in organic aerosols in anthropogenically-influenced northern hemisphere mid-latitudes, *Geophys. Res. Lett.*, 34, L13801, doi:10.1029/2007GL029979, 2007
- 10 Zhang, Q., Jimenez, J., Canagaratna, M., Ulbrich, I., Ng, N., Worsnop, D., and Sun, Y.: Understanding atmospheric organic aerosols via factor analysis of aerosol mass spectrometry: a review, *Anal. Bioanal. Chem.*, 401, 3045–3067, doi:10.1007/s00216-011-5355-y, 2011.
- 15

## SOA from aqueous reactions of phenols with two oxidants

L. Yu et al.

**Table 1.** Summary of the chemical characteristics of phenolic aqSOA formed under different experimental conditions.

| Sample information   |                             | AMS results          |       |      |      |                              |                             |                           | Nano-DESI MS results           |                          | IC results                               | TOC results                                    |     |
|--|-----------------------------|----------------------|-------|------|------|------------------------------|-----------------------------|---------------------------|--------------------------------|--------------------------|--|--|-----|
| Precursor  | Oxidant                     | $t_{1/2}^a$<br>(min) | OM/OC | O/C  | H/C  | OS <sub>C</sub> <sup>b</sup> | $\sum m/z \geq 80^c$<br>(%) | Dimer <sup>d</sup><br>(%) | # of<br>molecules <sup>e</sup> | # of common<br>molecules | Organic acids<br>(% of TOC) <sup>f</sup> | Dissolved volatile<br>species <sup>g</sup> (%) |     |
| Syringol<br>(C <sub>8</sub> H <sub>10</sub> O <sub>3</sub> ) | <sup>3</sup> C <sup>*</sup> | 16                   | 2.29  | 0.85 | 1.66 | 0.04                         | 13.3                        | –                         | 1156                           | 883                      | 0.8                                      | 6.6  |     |
|  | ·OH                         | 45                   | 2.27  | 0.86 | 1.64 | 0.08                         | 12.3                        | –                         | 998                            |                          | 0.7                                      | 5.9  |     |
| Guaiacol<br>(C <sub>7</sub> H <sub>8</sub> O <sub>2</sub> )  | <sup>3</sup> C <sup>*</sup> | 35                   | 2.37  | 0.92 | 1.79 | 0.05                         | 14.7                        | 0.70                      | 827                            |                          | 643                                      | 0.8  | 4.6 |
|  | ·OH                         | 160                  | 2.72  | 1.18 | 1.85 | 0.51                         | 9.8                         | 0.15                      | 871                            |                          |  | 2.2  | 2.7 |
| Phenol<br>(C <sub>6</sub> H <sub>6</sub> O)                  | <sup>3</sup> C <sup>*</sup> | 480                  | 2.63  | 1.11 | 1.70 | 0.52                         | 8.8                         | 0.51                      | 721                            | 209                      |  | 2.1  | 2.8 |
|  | ·OH                         | 672                  | 2.79  | 1.23 | 1.72 | 0.74                         | 6.8                         | 0.01                      | 445                            |                          |  | 3.8  | 5.7 |

<sup>a</sup>  $t_{1/2}$  is the time when approximately half of the phenolic precursor was reacted (as monitored by HPLC/UV-vis).<sup>b</sup> OS<sub>C</sub> indicates the oxidation state of the carbon atom (= 2 × O/C – H/C)<sup>c</sup> % of total ion signal at  $m/z \geq 80$  in the AMS spectra.<sup>d</sup> Estimated based on the signal contribution of the molecular ions of the dimers in the AMS spectra and the NIST spectra. NIST spectrum of syringol dimer is not available.<sup>e</sup> Total number of molecules identified in the (+) ion mode and (–) ion mode nano-DESI MS spectra.<sup>f</sup> % of organic carbon mass in aqSOA accounted for by the sum of 8 organic acids (formate, acetate, pyruvate, malate, oxalate, malonate, fumarate, and mealmate).<sup>g</sup> Dissolved volatile species is calculated as the differences in TOC between flash-frozen and blown-down samples after correction for the mass of unreacted precursors.

Title Page

Abstract

Introduction

Conclusions

References

Tables

Figures



Back

Close

Full Screen / Esc

Printer-friendly Version

Interactive Discussion



## SOA from aqueous reactions of phenols with two oxidants

L. Yu et al.

Title Page

Abstract

Introduction

Conclusions

References

Tables

Figures



Back

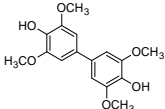
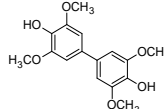
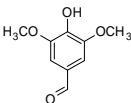
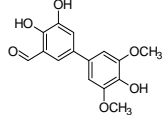
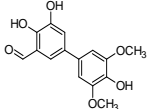
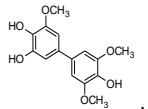
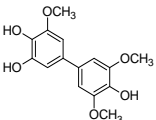
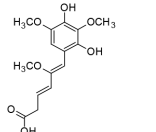
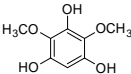
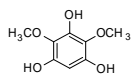
Close

Full Screen / Esc

Printer-friendly Version

Interactive Discussion

**Table 2.** Top 10 most abundant compounds in syringol SOA formed in  $^3\text{C}^*$ - and  $\cdot\text{OH}$ -mediated reactions identified with (–) nano-DESI MS.

| $^3\text{C}^*$ reaction |  |   | $\cdot\text{OH}$ reaction |  |  |     |
|-------------------------|--|---|---------------------------|--|--|-----|
| No.                     | Molecular formula*                                   | Proposed structure  | DBE                       | Molecular formula*                                   | Proposed structure   | DBE |
| 1                       | $\text{C}_{16}\text{H}_{18}\text{O}_6$<br>(306.1103) |  | 8                         | $\text{C}_{16}\text{H}_{18}\text{O}_6$<br>(306.1103) |  | 8   |
| 2                       | $\text{C}_9\text{H}_{10}\text{O}_4$<br>(182.0579)    |  | 5                         | $\text{C}_{15}\text{H}_{14}\text{O}_6$<br>(290.0790) |  | 9   |
| 3                       | $\text{C}_{15}\text{H}_{14}\text{O}_6$<br>(290.0790) |  | 9                         | $\text{C}_{15}\text{H}_{16}\text{O}_6$<br>(292.0946) |  | 8   |
| 4                       | $\text{C}_{15}\text{H}_{16}\text{O}_6$<br>(292.0946) |  | 8                         | $\text{C}_{15}\text{H}_{18}\text{O}_7$<br>(310.1052) |  | 7   |
| 5                       | $\text{C}_8\text{H}_{10}\text{O}_5$<br>(186.0528)    |  | 4                         | $\text{C}_8\text{H}_{10}\text{O}_5$<br>(186.0528)    |  | 4   |

\* Molecular formula of top 10 most abundant compounds with their exact mass in the parenthesis.

## SOA from aqueous reactions of phenols with two oxidants

L. Yu et al.

Title Page

Abstract

Introduction

Conclusions

References

Tables

Figures



Back

Close

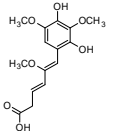
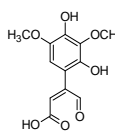
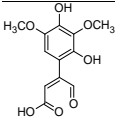
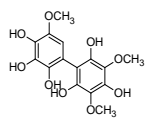
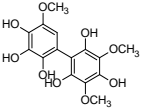
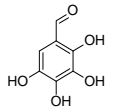
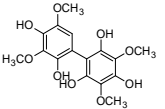
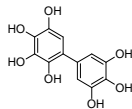
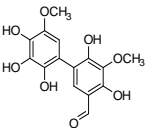
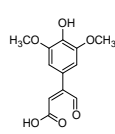
Full Screen / Esc

Printer-friendly Version

Interactive Discussion



Table 2. Continued.

| $^3\text{C}^+$ reaction |  |   | $\cdot\text{OH}$ reaction |  |  |     |
|-------------------------|--|---|---------------------------|--|--|-----|
| No.                     | Molecular formula*                                   | Proposed structure  | DBE                       | Molecular formula*                                   | Proposed structure   | DBE |
| 6                       | $\text{C}_{15}\text{H}_{18}\text{O}_7$<br>(310.1052) |  | 7                         | $\text{C}_{12}\text{H}_{12}\text{O}_7$<br>(268.0583) |   | 7   |
| 7                       | $\text{C}_{12}\text{H}_{12}\text{O}_7$<br>(268.0583) |  | 7                         | $\text{C}_{15}\text{H}_{16}\text{O}_9$<br>(340.0794) |  | 8   |
| 8                       | $\text{C}_{15}\text{H}_{16}\text{O}_9$<br>(340.0794) |  | 8                         | $\text{C}_7\text{H}_6\text{O}_5$<br>(170.0215)       |   | 5   |
| 9                       | $\text{C}_{16}\text{H}_{18}\text{O}_9$<br>(354.0950) |  | 8                         | $\text{C}_{12}\text{H}_{10}\text{O}_7$<br>(266.0426) |  | 8   |
| 10                      | $\text{C}_{15}\text{H}_{14}\text{O}_8$<br>(322.0688) |  | 9                         | $\text{C}_{12}\text{H}_{12}\text{O}_6$<br>(252.0634) |   | 7   |

\* Molecular formula of top 10 most abundant compounds with their exact mass in the parenthesis.

## SOA from aqueous reactions of phenols with two oxidants

L. Yu et al.

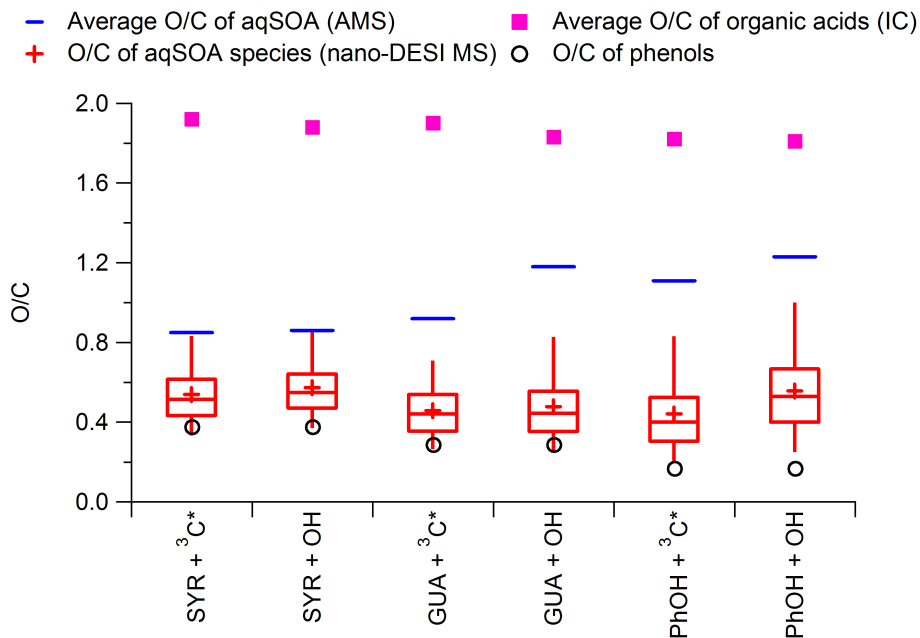


**Figure 1.** The average O/C ratios of aqSOA formed from the reactions of syringol (SYR), guaiacol (GUA), and phenol (PhOH) with <sup>3</sup>C\* and ·OH, respectively determined by AMS (blue bars) and the average O/C of organic acids determined by IC (pink squares). The distributions of the O/C of individual molecules in the aqSOA determined by nano-DESI MS are shown in box plots, in which the whiskers above and below the boxes indicate the 95th and 5th percentiles, the upper and lower boundaries of the boxes indicate the 75th and 25th percentiles, and the lines in the boxes indicate the median values and the cross symbols indicate the mean values. The O/C of the precursors are shown as black circles.

Title Page

Abstract

Introduction

Conclusions

References

Tables

Figures



Back

Close

Full Screen / Esc

Printer-friendly Version

Interactive Discussion



## SOA from aqueous reactions of phenols with two oxidants

L. Yu et al.

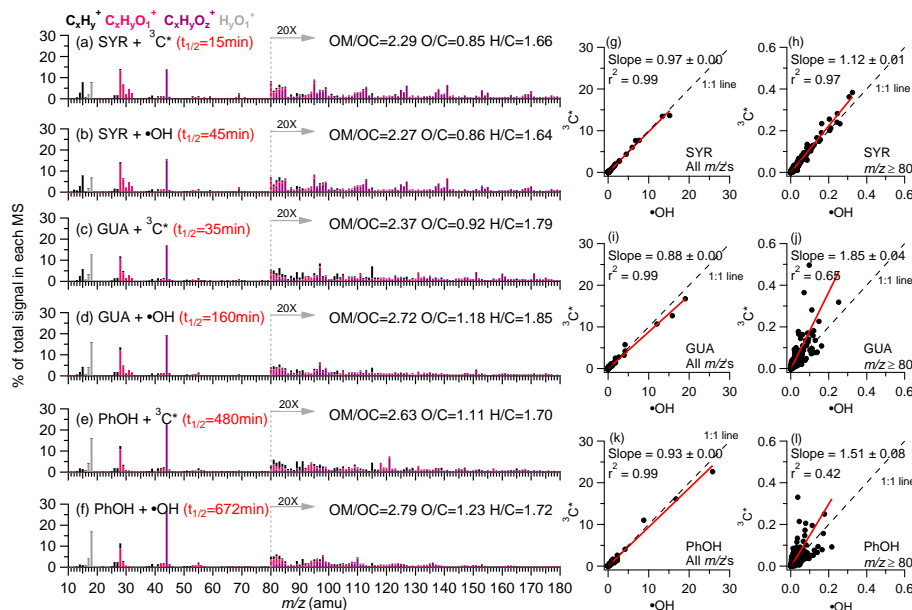


**Figure 2.** AMS spectra of aqSOA formed from the reactions of (a–b) syringol (SYR), (c–d) guaiacol (GUA), and (e–f) phenol (PhOH) with  $^3\text{C}^*$  and  $\cdot\text{OH}$ , respectively. The peaks are color-coded according to four ion categories:  $\text{C}_x\text{H}_y^+$ ,  $\text{C}_x\text{H}_y\text{O}_1^+$ ,  $\text{C}_x\text{H}_y\text{O}_2^+$ , and  $\text{H}_y\text{O}_1^+$  ( $x \geq 1$ ;  $y \geq 0$ ;  $z \geq 2$ ). The ion signals at  $m/z \geq 80$  are enhanced by a factor of 20 for clarity. The photoreaction time and the elemental ratios of the aqSOA are shown in the legends. Scatter plots that compare the mass spectra of aqSOA formed from two different oxidants for all  $m/z$ 's (g, i, k) and for  $m/z \geq 80$  (h, j, l) were performed using the orthogonal distance regression (ODR). The linear regression slopes and correlation coefficients are shown in the legends.

Title Page

Abstract

Introduction

Conclusions

References

Tables

Figures



Back

Close

Full Screen / Esc

Printer-friendly Version

Interactive Discussion







## SOA from aqueous reactions of phenols with two oxidants

L. Yu et al.

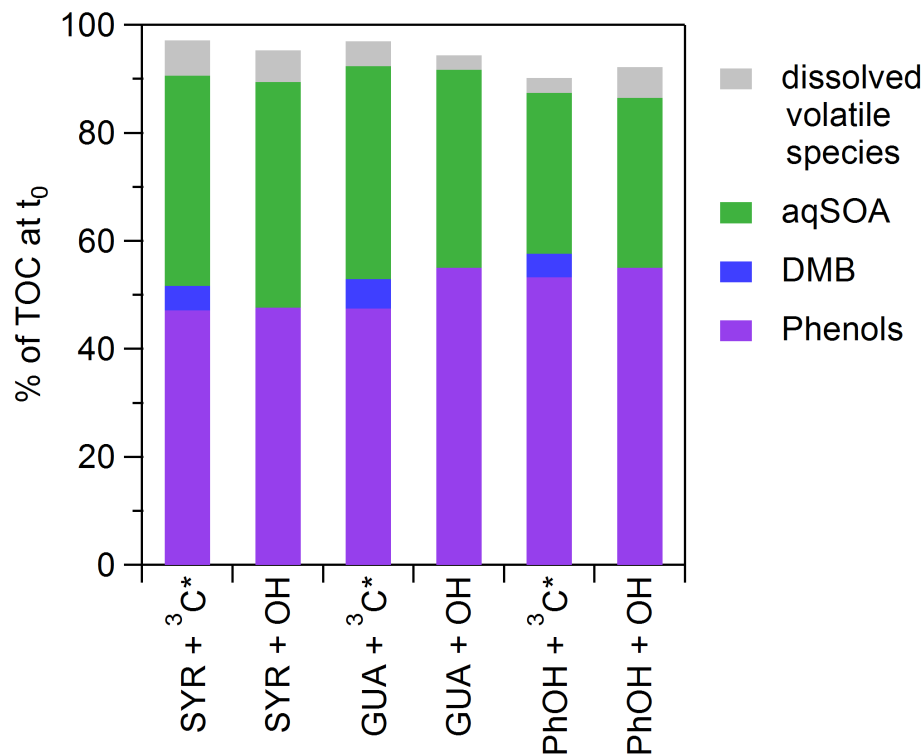


**Figure 4.** Contributions of reactants (phenolic precursor and DMB) and products (dissolved volatile species and aqSOA) to the solution TOC after illumination to  $t_{1/2}$ . TOC amounts are expressed relative to the TOC in the initial solution prior to illumination (i.e., at  $t_0$ ).

|                          |              |
|--------------------------|--------------|
| Title Page               |              |
| Abstract                 | Introduction |
| Conclusions              | References   |
| Tables                   | Figures      |
| ◀                        | ▶            |
| ◀                        | ▶            |
| Back                     | Close        |
| Full Screen / Esc        |              |
| Printer-friendly Version |              |
| Interactive Discussion   |              |



## SOA from aqueous reactions of phenols with two oxidants

L. Yu et al.

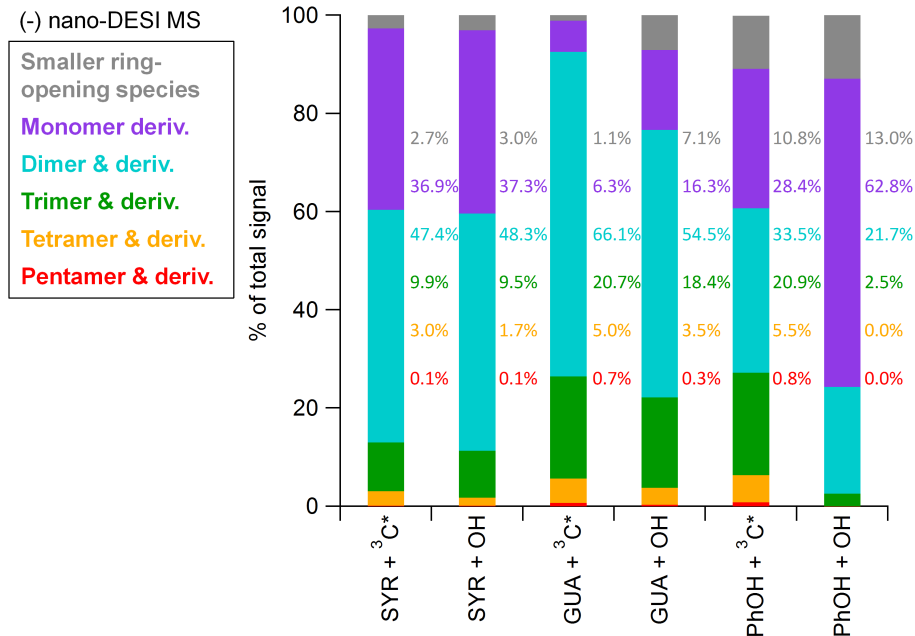


**Figure 5.** The signal weighted distributions of syringol (SYR), guaiacol (GUA) and phenol (PhOH) aqSOA formed in  $^3\text{C}^*$ - and  $\cdot\text{OH}$ -mediated reactions, respectively, based on the degree of oligomerization. The data are from the (-) nano-DESI MS spectra. Note that hexamer and derivatives are only found in (+) nano-DESI MS spectrum for GUA aqSOA initiated with  $^3\text{C}^*$  and (-) nano-DESI MS spectrum for PhOH aqSOA initiated with  $^3\text{C}^*$ . The numbers indicate the contributions of individual categories to the total signals for each sample.

## SOA from aqueous reactions of phenols with two oxidants

L. Yu et al.

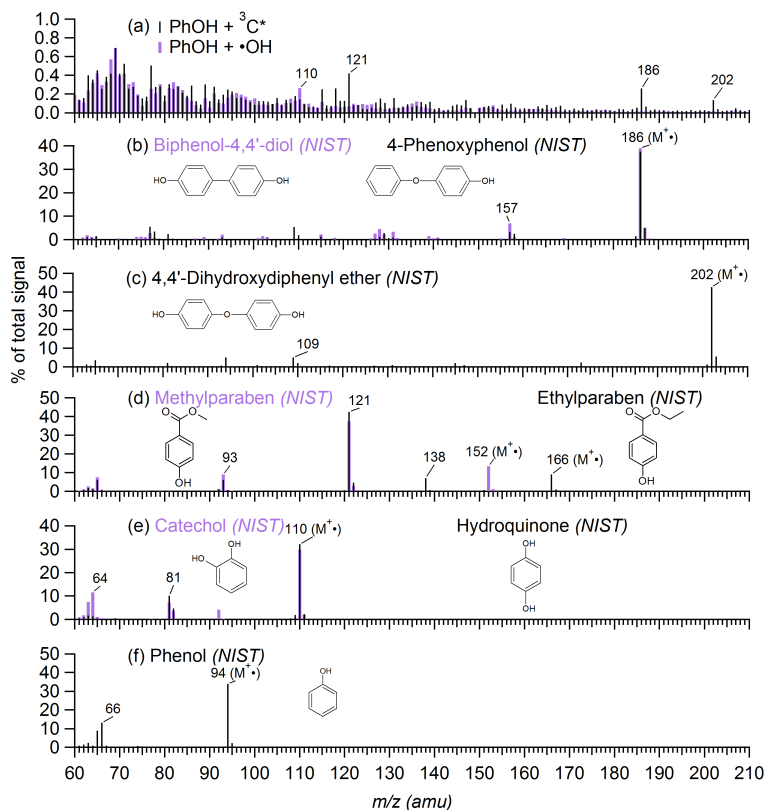


**Figure 6.** Comparisons between (a) the AMS mass spectra (in integer  $m/z$ ) of phenol (PhOH) aqSOA formed via reactions with  $^3\text{C}^*$  and  $\cdot\text{OH}$ , respectively, and the NIST mass spectra of (b) biphenol-4,4'-diol and 4-phenoxyphenol, (c) 4,4'-dihydroxydiphenyl ether, (d) methylparaben and ethylparaben, (e) catechol and hydroquinone, and (f) phenol. The chemical structures for each compound are shown and the molecular ions ( $\text{M}^+$ ) are marked.

## SOA from aqueous reactions of phenols with two oxidants

L. Yu et al.

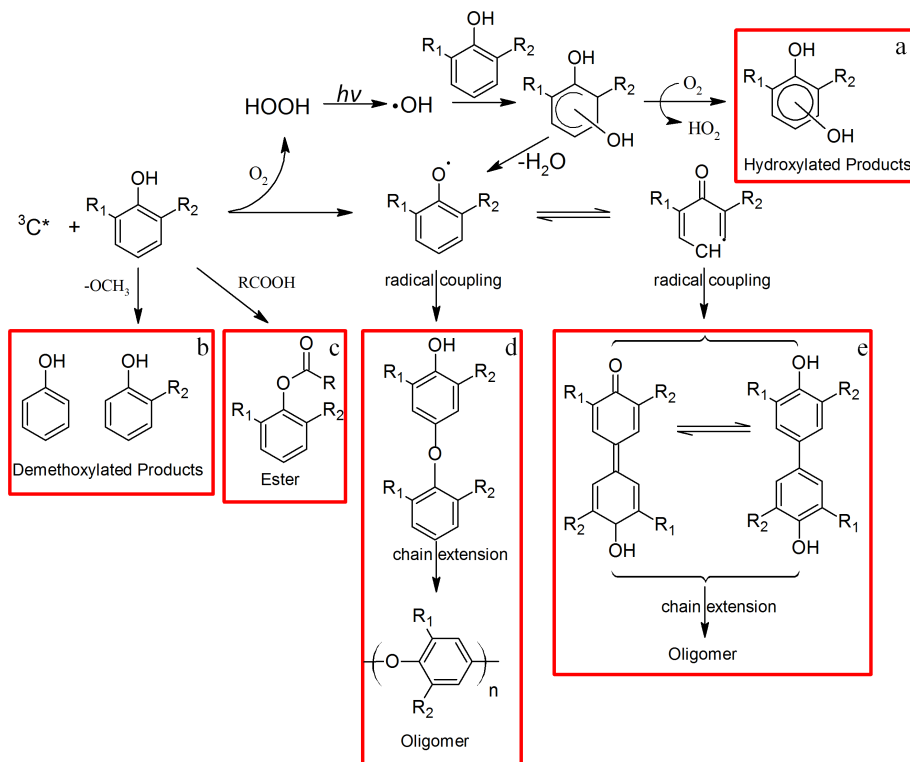


**Figure 7.** A schematic illustrates the formation of hydroxylated species, dimers and higher oligomers, esters, and demethoxylated products from aqueous photooxidation of phenolic compounds. Species produced via pathways (a–e) may undergo further ring-opening processes to form ketones and carboxylic acids. Phenol:  $R_1 = H$ ,  $R_2 = H$ ; Guaiacol:  $R_1 = OCH_3$ ,  $R_2 = H$ ; Syringol:  $R_1 = OCH_3$ ,  $R_2 = OCH_3$ . Note that while radical coupling here is shown through the carbon opposite (para) the phenoxy group, other geometric isomers will also be formed during these reactions.

Title Page

Abstract

Introduction

Conclusions

References

Tables

Figures



Back

Close

Full Screen / Esc

Printer-friendly Version

Interactive Discussion



## SOA from aqueous reactions of phenols with two oxidants

L. Yu et al.

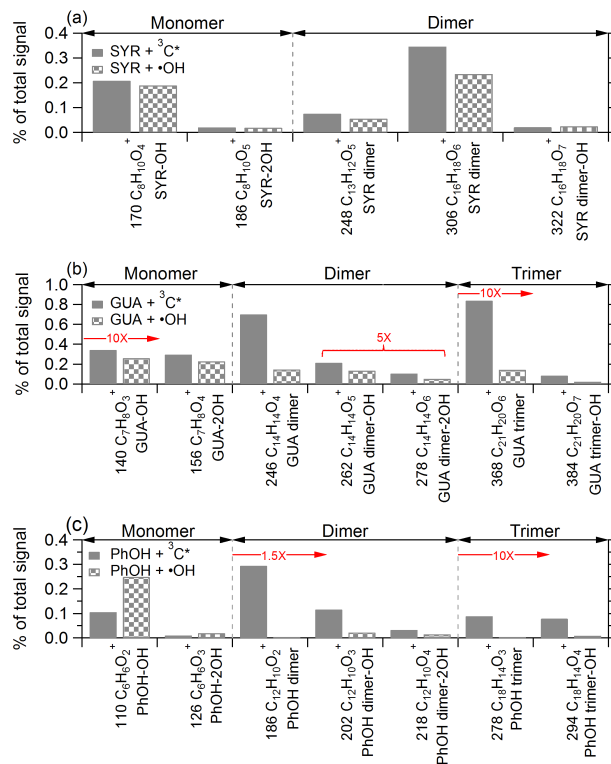


**Figure 8.** Comparisons of the relative abundances of signature ions in the AMS spectra of the aqSOA of (a) syringol (SYR), (b) guaiacol (GUA), and (c) phenol (PhOH) produced from <sup>3</sup>C\* and ·OH-mediated reactions. The signal contributions of certain signature ions are enhanced for clarity. The *m/z* values of the signature ions are shown in front of the ion formula in the *x* axes. Identities of possible parent compounds are shown to the right. 2OH represents 2 additional hydroxyl groups attached to the aromatic ring.

|                          |              |
|--------------------------|--------------|
| Title Page               |              |
| Abstract                 | Introduction |
| Conclusions              | References   |
| Tables                   | Figures      |
| ◀                        | ▶            |
| ◀                        | ▶            |
| Back                     | Close        |
| Full Screen / Esc        |              |
| Printer-friendly Version |              |
| Interactive Discussion   |              |

## SOA from aqueous reactions of phenols with two oxidants

L. Yu et al.

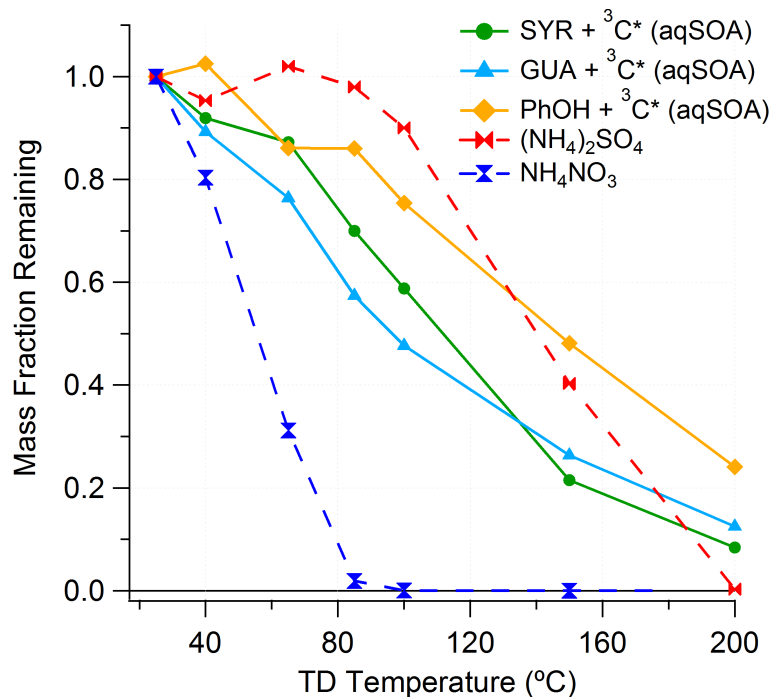


**Figure 9.** Mass thermograms of ammonium sulfate ((NH<sub>4</sub>)<sub>2</sub>SO<sub>4</sub>), ammonium nitrate (NH<sub>4</sub>NO<sub>3</sub>), syringol (SYR), guaiacol (GUA) and phenol (PhOH) aqSOA formed in <sup>3</sup>C\*-mediated aqueous-phase reactions.

[Title Page](#)[Abstract](#)[Introduction](#)[Conclusions](#)[References](#)[Tables](#)[Figures](#)[◀](#)[▶](#)[◀](#)[▶](#)[Back](#)[Close](#)[Full Screen / Esc](#)[Printer-friendly Version](#)[Interactive Discussion](#)

## SOA from aqueous reactions of phenols with two oxidants

L. Yu et al.

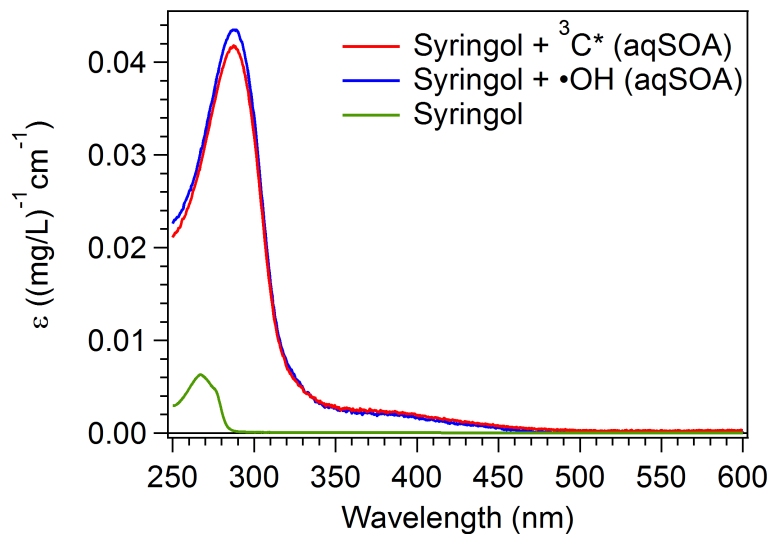


**Figure 10.** UV-vis spectra of syringol and syringol aqSOA formed in <sup>3</sup>C\* - and ·OH-mediated aqueous-phase reactions. The aqSOA spectra were corrected for absorbance contributions from unreacted reactants (syringol and DMB).

[Title Page](#)[Abstract](#)[Introduction](#)[Conclusions](#)[References](#)[Tables](#)[Figures](#)[⏪](#)[⏩](#)[◀](#)[▶](#)[Back](#)[Close](#)[Full Screen / Esc](#)[Printer-friendly Version](#)[Interactive Discussion](#)